Investigation of the Ground State Features of Some Excotic Nuclei by Using Effective Skyrme Interaction

Hüseyin AYTEKİN[1], Eyyüp TEL[2] and Rıdvan BALDIK[1]

[1]*Department of Physics, Zonguldak Karaelmas University, 67100, Zonguldak-TURKEY*
[2]*Department of Physics, Gazi University, 06500, Ankara-TURKEY*
e-mail: huseyinaytekin@gmail.com • aytekin@karaelmas.edu.tr

Abstract

Nuclear many-body system is usually described through a mean-field built upon a nucleon-nucleon effective interaction. This interaction has been developed over the years for both stable and unstable nuclei as precise spectroscopic data has been built up. In this study, the proton and neutron densities, charge densities, root mean square (rms) nuclear charge radii, rms nuclear mass radii, rms nuclear proton and neutron radii, and neutron skin thickness were calculated for the neutron-rich Ni, Kr and Sn isotopes by the Hartree-Fock method with an effective Skyrme force based on nucleon-nucleon interactions known as SI, SIII, SVI, T3, SKM and SKM*. The results obtained via theoretical approach are close to experimental observations.

Key Words: Hartree-Fock calculations, nucleon–nucleon interactions, charge distribution.
PACS: 21.60. Jz, 13.75.Cs., 21.10.Ft

1. Introduction

The scattering of particles and ions from nuclei has provided over the years invaluable information on charge, matter, current, and momentum distributions of stable nuclei on and near the stability line. Recent development of radioactive isotope beam techniques has opened a new field for the study of unstable nuclei far from the stability line [1, 2, 3]. As a result, our knowledge of nuclear physics has been extended from stable nuclei to unstable nuclei. Experiments with radioactive isotope beams have already shown that the properties of unstable nuclei are quite different from those of stable ones [4]. Therefore, it is very interesting to investigate the properties of unstable nuclei theoretically with reliable theories and models. The results will provide references for future experiments as well as tests of reliability of the well-established nuclear theory for unstable nuclei.

Most exotic nuclei, which have an extraordinary ratio of protons and neutrons (the proton-rich, or the neutron-rich) and short lived species, cannot be used as targets at rest. Instead, direct reaction with radioactive isotope beam can be done in inverse kinematics, where the role of beam and target are interchanged. The charge and matter distributions of these nuclei were tested in analyses of differential and total reaction cross section of proton scattering on exotic nuclei, using different phenomenological and theoretical methods. Concerning the charge distributions of nuclei, it is known that their most accurate determination can be obtained from electron-nucleus scattering. For the case of exotic nuclei, the corresponding charge densities are planned to be obtained by colliding electrons with these nuclei in storage rings [5].

Nuclear charge density distribution is one of the basic quantities describing nuclear properties. Charge densities can give us much detailed information about the internal structure of nuclei, as they are directly related to the wave functions of protons, which are important keys in many nuclear physics calculations. Charge density distributions for stable nuclei have been well studied with some methods [6–8]. For unstable nuclei, although studies of electron scattering have not yet been realized, nuclear physicists have already planned to explore the structures of unstable nuclei with electron-nucleus scattering. Based on new techniques for producing high-quality radioactive isotope beams, new electron-nucleus colliders are now under construction at RIKEN in Japan [9] and at GSI in Germany [10]. Therefore it is expected that information on charge density distributions of unstable nuclei will soon be available.

In this study, charge densities, proton and neutron densities and rms radii of several unstable isotopes of medium (i.e. Ni, Kr) and heavy (i.e. Sn) nuclei are calculated. The isotopes of Ni and Sn are chosen because they have been as first candidates accessible for charge densities and rms radii determination and as key isotopes for structure studies of unstable nuclei at the electron-radioactive-ion collider in RIKEN [11].

The Hartree-Fock method with Skyrme force is widely used for studying the properties of nuclei. This method is successfully used for a wide range of nuclear characteristics such as binding energy, rms charge radii, neutron and proton density, electromagnetic multipole moments, etc. In this study, by using Hartree-Fock approximation with effective Skyrme force, charge rms radii, neutron rms radii, neutron and proton density were calculated for Ni, Kr and Sn isotopes nuclei. The calculated results were compared with the experimental and theoretical calculations of the liquid-drop model.

2. Hartree-Fock Calculations via Effective Skyrme Forces

The Hartree-Fock equations are derived variationally from the total energy functional of the nucleus:

$$E = E_{\text{Skyrme}} + E_{\text{Coulomb}} + E_{\text{pair}} - E_{\text{cm}}. \tag{1}$$

Here, E is the total energy of nucleus, E_{Skyrme} is the energy of Skyrme interaction, $E_{Coulomb}$ is the Coulomb interaction energy, E_{pair} is the two-nucleon interaction pairing energy and E_{cm} is the energy for correction for the spurious center-of-mass motion of the mean field [12].

As early as the 1950s, Skyrme proposed a phenomenological nuclear force, which is now called the conventional Skyrme force. This force consists of some two-body terms together with a three-body term [13]:

$$V_{CS} = \sum_{i<j} V_{ij}^{(2)} + \sum_{i<j<k} V_{ijk}^{(3)}. \tag{2}$$

Providing simultaneously reasonable excited state as well as ground state properties, modifications and generalizations to the conventional Skyrme force have been proposed since the 1970s. Vauthering and Brink were determined two sets of conventional Skyrme force parameters (so-called SI and SIII) by fitting experimental binding energies, nucleon densities and root mean square radii. Another set of modified Skyrme forces (SKM) given by Brack et al. [14] is based on fitting the fission barriers of heavy deformed nuclei; and is denoted by SKM*. An extended Skyrme force can be written

$$
\begin{aligned}
V_{\text{Skyrme}} \quad = \quad & t_0(1 + x_0 P_\sigma)\delta(\vec{r}) + \tfrac{1}{2}t_1(1 + x_1 P_\sigma)\left\{\delta(\vec{r})\,\vec{k}^2 + \vec{k}'^2\delta(\vec{r}))\right\} + \\
& t_2(1 + x_2 P_\sigma)\vec{k}' \cdot \delta(\vec{r})\,\vec{k} + \tfrac{1}{6}t_3(1 + x_3 P_\sigma)\rho\alpha(\vec{R})\delta(\vec{r}) + it_4\vec{k}' \cdot \delta(\vec{r})(\vec{\sigma}_i + \vec{\sigma}_j) \times \vec{k},
\end{aligned}
\tag{3}
$$

where $\vec{k}$ is the relative momentum, $\delta(\vec{r})$ is the delta function, P_σ is the space exchange operator, $\vec{\sigma}$ is the vector of Pauli spin matrices and t_o, t_1, t_2, t_3, t_4, x_o, x_1, x_2, x_3, α are Skyrme force parameters. These Skyrme force parameters are given in Table 1. The values of these parameters and the other Skyrme force parameters can be found in reference [15].

Table 1. Skyrme force parameters [15].

Force	SI	SIII	SVI	T3	SKM	SKM*
$t_0(\text{MeV}\cdot\text{fm}^3)$	-1057.3	-1128.75	-1101.81	-1791.80	-2645.0	-2645.0
$t_1(\text{MeV}\cdot\text{fm}^5)$	235.9	395.0	271.67	298.50	385.0	410.0
$t_2(\text{MeV}\cdot\text{fm}^5)$	-100.0	-95.0	-138.33	-99.50	-120.0	-135.0
$t_3(\text{MeV}\cdot\text{fm}^{3\alpha})$	14463.5	14000.0	17000.0	12794.0	15595.0	15595.0
$t_4(\text{MeV}\cdot\text{fm}^5)$	0	120	115	126	130	130
x_0	0.56	0.45	0.583	0.138	0.09	0.09
x_1	0.0	0.0	0.0	-1.0	0.0	0.0
x_2	0.0	0.0	0.0	1.0	0.0	0.0
x_3	1.0	1.0	1.0	0.075	0.0	0.0
α	1.0	1.0	1.0	1/3	1/6	1/6

The Coulomb interaction is a well known piece of the nuclear interaction. Infinite range of this interaction makes it very consuming to evaluate the exchange part exactly and makes the exchange contribution only a small fraction of the total Coulomb energy [12].

In the direct term, the nuclear charge distribution includes in folding with the finite size of the proton. The mean field, however, localizes the nucleus and thus breaks translational invariance, so that the center-of-mass of the whole nucleus can oscillate in the mean field. In principle, one should project a state with good total momentum zero out of the given mean-field state. A simple and reliable substitute for the projection is to subtract the zero point energy of the nearly harmonic oscillations of the center of mass [16, 17]. The correction is

$$E_{\text{cm}} = \frac{< P_{\text{cm}}^2 >}{2Am}. \tag{4}$$

An even simpler approach to the center-of-mass correction was used in early applications. One can take the one-body part of equation (4), $P_{\text{cm}}^2 = \sum_i p_i^2$, and thus express center-of-mass correction as a modification of the nucleon mass

$$\frac{\hbar^2}{2m} \rightarrow \frac{\hbar^2}{2m}\left(1 - \frac{1}{A}\right). \tag{5}$$

The pairing energy is given by

$$E_{\text{pair}} = \sum_q G_q \left[\sum \sqrt{w_\beta(1-w_\beta)}\right]^2, \tag{6}$$

where G_q and w_β are the pairing matrix elements and the pairing weights of the proton and neutron, respectively. The BCS (Bardeen-Cooper-Schrieffer) equations for the pairing weights w_β are obtained by varying the energy functional (equation 1) with respect to w_β. This yields the standard BCS equations for the case of a constant pairing force. The occupation weights become

$$w_\beta = \frac{1}{2}\left(1 - \frac{\varepsilon_\beta - \varepsilon_{F,q}}{\sqrt{(\varepsilon_\beta - \varepsilon_{F,q})^2 + \Delta_q^2}}\right). \tag{7}$$

The pairing gap Δ_q and Fermi energy $\varepsilon_{F,q}$ are obtained by simultaneous of the gap equation is

$$\frac{\Delta_q}{G_q} = \sum_{\beta\varepsilon q} \sqrt{w_\beta(1-w_\beta)}, \tag{8}$$

and the particle-number condition is

$$A_q = \sum_{\beta\in q} w_\beta, \tag{9}$$

where A_q is the desired number of protons ($q = pr$) or neutrons ($q = ne$).

The pairing effects in the BCS (Bardeen-Cooper-Schrieffer) formalism in the approximation constant-force with $G_{pr} = \frac{22 \text{MeV}}{A}$, $G_{ne} = \frac{29 \text{MeV}}{A}$ where A is the total nucleon number of a nucleus. A commonly accepted parameterization of gap is $\nabla_q = 11.2 \text{ MeV} / \sqrt{A}$, and $A = A_{Pr} + A_{ne}$ is the total nucleon number.

The neutron, proton or charge densities are given by

$$\rho_q(\vec{r}) = \sum_{\beta \in q} w_\beta \psi_\beta(\vec{r})^+ \psi_\beta(\vec{r}), \tag{10}$$

where q is used for neutron, proton and charge densities and ψ_β is the single-particle wave function of the state β, the occupation probability of the state β is denoted by $w_\beta \cdot w_\beta = 1$ for completely filled shells, but fractional occupancies occur for nonmagic nuclei: these are determined by pairing scheme [17].

The rms radii of neutron, proton, charge and mass densities can be evaluated by using equation (10) with the following formula

$$r_q = \left\langle r_q^2 \right\rangle^{1/2} = \left[\frac{\int r^2 \rho_q^(r) dr}{\int \rho_q^(r) dr} \right]^{1/2}. \tag{11}$$

A quantity of both theoretical and experimental interest, the neutron skin thickness t, can then be defined as the difference between the neutron rms radius and the proton rms radius as

$$t = r_n - r_p. \tag{12}$$

3. Results and Discussions

In this study, we have calculated the rms nuclear charge radii, rms nuclear mass radii, and the radii of proton and neutron for Ni, Kr and Sn isotopes by using the Hartree-Fock method with an effective interaction with Skyrme forces parameters (Table 1) in SI, SIII, SVI, T3, SKM and SKM* interactions. We have used the Skyrme interaction parameters given in Table 1 for calculations with the program HAFOMN [18]. For description of the systems consisting of an odd number of particles, the filling approximation has been used. The Hartree-Fock and pairing equations are coupled, and they are solved by simultaneous iteration of the wave functions and the occupation weights w_β. Completely filled shells have $w_\beta = 1$, but fractional occupancies occur for nonmagic nuclei; these are determined by a pairing scheme discussed in detail in references [17, 19, 20].

We have calculated charge density distribution, proton and neutron densities distributions and neutron skin thickness in SKM*. We have compared the calculated rms nuclear charge radii for the Ni, Kr and Sn isotopes with experimental data in Table 2, and the calculated rms nuclear mass radii are shown in Table 3. The proton and neutron radii are given in Tables 4 and 5. The charge densities distributions, proton and neutron charge densities, have drawn in the Figures 1, 2, 3 and 4.

The rms radii of neutron, proton, charge and mass distributions can be evaluated from densities equations (10)–(11). In this study, we have calculated the nuclear charge rms radii values by using the Hartree-Fock method with an effective interaction with Skyrme forces parameters given in Table 1 for Ni, Kr and Sn isotopes, and the obtained results have also been compared with experimental data. Our comparison is found in Table 2. Theoretically the calculated charge rms values are quite consistent with the theoretical calculations using the Skyrme forces parameters in Table 2. Also in Table 2, are the nuclear charge rms values, calculated by using Skyrme forces, compared with the values of radius $r_o A^{1/3}$ in the liquid-drop model, in which the number of nucleons per unit volume is roughly constant.

Table 2. Calculated rms Nuclear Charge Radii (in fm) and $r_0 = 1.3$ fm (experimental data: I. Angeli, Atom. Dat. Nucl. Dat. Tab., 2004 [21]).

Isotopes	SI	SIII	SVI	T3	SKM	SKM*	Experiment	$r_0 A^{1/3}$
$^{58}Ni_{30}$	3.721	3.839	3.841	3.795	**3.789**	3.811	3.7748±0.0014	5.032
$^{60}Ni_{32}$	3.744	3.862	3.865	**3.810**	3.805	3.827	3.8119±0.0014	5.089
$^{61}Ni_{33}$	3.757	3.874	3.877	**3.820**	3.816	3.837	3.8221±0.0017	5.117
$^{62}Ni_{34}$	3.769	3.886	3.890	3.830	3.828	**3.849**	3.8406±0.0016	5.145
$^{64}Ni_{36}$	3.794	3.910	3.915	3.852	**3.854**	3.874	3.8587±0.0017	5.200
$^{74}Ni_{46}$	3.886	3.999	4.007	3.938	3.944	3.963		5.458
$^{78}Ni_{50}$	3.915	4.026	4.035	3.966	3.969	3.987		5.554
$^{82}Kr_{46}$	4.094	4.210	4.217	4.152	4.164	**4.183**	4.1922±0.0015	5.648
$^{92}Kr_{56}$	4.168	**4.290**	4.297	4.213	4.220	4.239	4.2732±0.0099	5.869
$^{94}Kr_{58}$	4.187	**4.309**	4.317	4.230	4.237	4.256	4.3014±0.0128	5.911
$^{109}Sn_{59}$	4.496	4.628	4.635	4.551	4.555	**4.574**	4.5690±0.0025	6.210
$^{111}Sn_{61}$	4.513	4.646	4.653	4.567	4.574	**4.592**	4.5859±0.0061	6.248
$^{121}Sn_{71}$	4.586	4.719	4.729	4.642	**4.652**	4.670	4.6589±0.0013	6.430
$^{124}Sn_{74}$	4.605	4.738	4.749	4.661	4.670	**4.688**	4.6759±0.0012	6.483
$^{125}Sn_{75}$	4.612	4.745	4.756	4.666	**4.675**	4.693	4.6779±0.0027	6.500

Table 3. Calculated Root-Mean-Square (RMS) Nuclear Mass Radii and $r_0 = 1.3$ fm.

Isotopes	SI	SIII	SVI	T3	SKM	SKM*	$r_0 A^{1/3}$
$^{58}Ni_{30}$	3.630	3.745	3.746	3.703	3.697	3.718	5.032
$^{60}Ni_{32}$	3.672	3.787	3.788	3.745	3.739	3.760	5.089
$^{61}Ni_{33}$	3.695	3.811	3.812	3.768	3.763	3.783	5.117
$^{62}Ni_{34}$	3.717	3.832	3.832	3.790	3.787	3.807	5.145
$^{64}Ni_{36}$	3.759	3.873	3.873	3.836	3.835	3.854	5.200
$^{74}Ni_{46}$	3.937	4.055	4.051	4.039	4.032	4.050	5.458
$^{78}Ni_{50}$	3.995	4.117	4.111	4.112	4.098	4.115	5.554
$^{82}Kr_{46}$	4.055	4.176	4.176	4.133	4.139	4.158	5.648
$^{92}Kr_{56}$	4.220	4.351	4.342	4.314	4.315	4.332	5.869
$^{94}Kr_{58}$	4.255	4.388	4.378	4.356	4.358	4.374	5.911
$^{109}Sn_{59}$	4.422	4.561	4.562	4.496	4.500	4.518	6.210
$^{111}Sn_{61}$	4.449	4.588	4.589	4.526	4.531	4.549	6.248
$^{121}Sn_{71}$	4.570	4.716	4.714	4.668	4.673	4.690	6.430
$^{124}Sn_{74}$	4.605	4.752	4.750	4.708	4.710	4.727	6.483
$^{125}Sn_{75}$	4.617	4.764	4.762	4.720	4.722	4.738	6.500

The value of r_o has been taken as 1.30 fm from electron scattering experiments. As with Hartree-Fock calculations with Skyrme forces, the radius values in liquid-drop model have increased from 5.03 fm (for ^{78}Ni) to 6.50 fm (for ^{125}Sn), depending on the mass number A for Ni, Kr and Sn isotopes. In the liquid-drop model calculations, radius values have increased faster than in the quantum mechanical Skyrme Hartree-Fock model. We have clearly shown that there are differences between the values calculated with quantum mechanical Skyrme Hartree-Fock model and $r_o A^{1/3}$ in the liquid-drop model. The experimental values for Ni, Kr and Sn isotopes nucleus are given in Table 2. The values calculated with quantum mechanical Skyrme Hartree-Fock model are closer from liquid-drop model to experimental values.
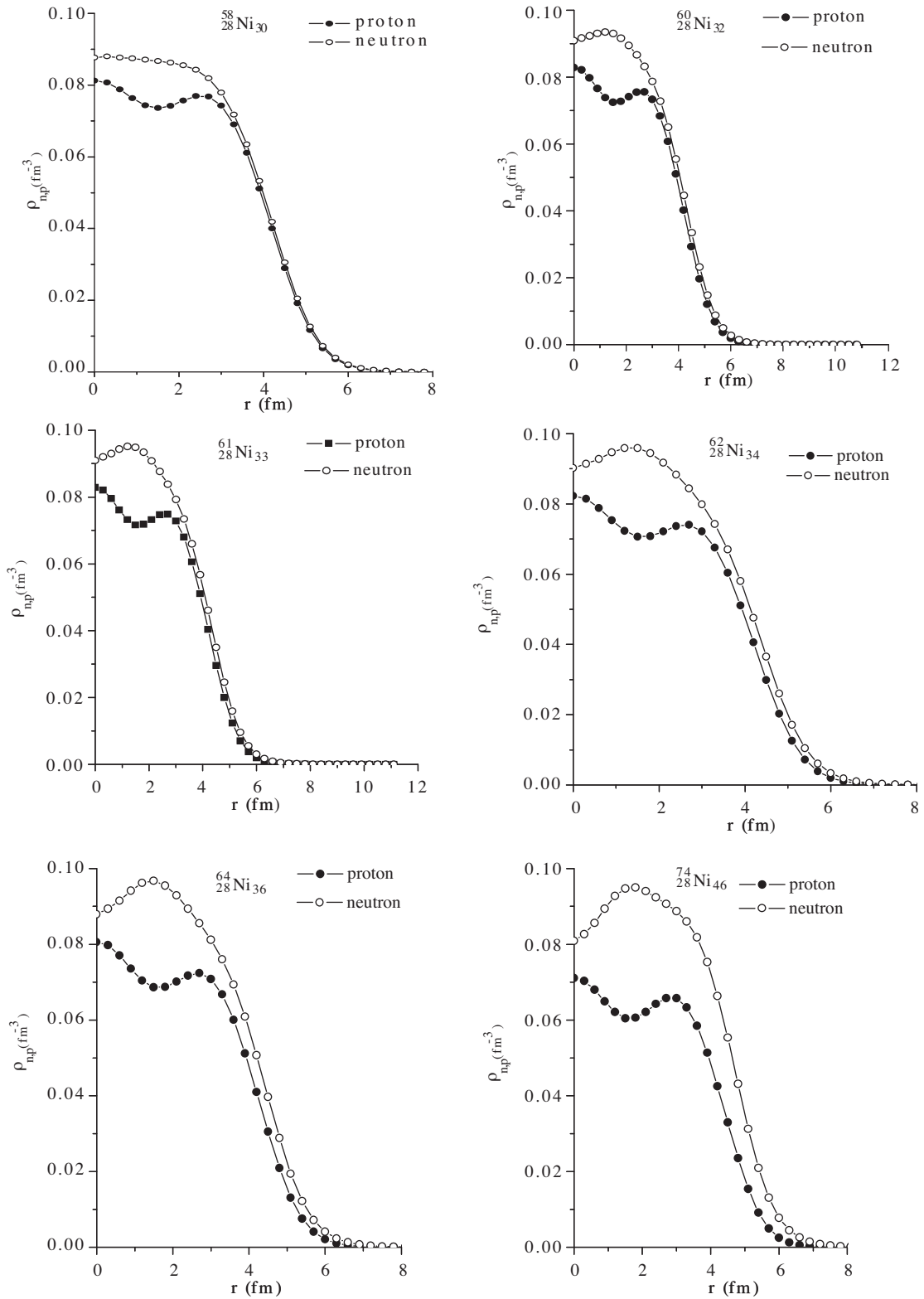
Figure 1. Comparison of calculated neutron and proton densities of Ni isotopes using the SKM* parameter.
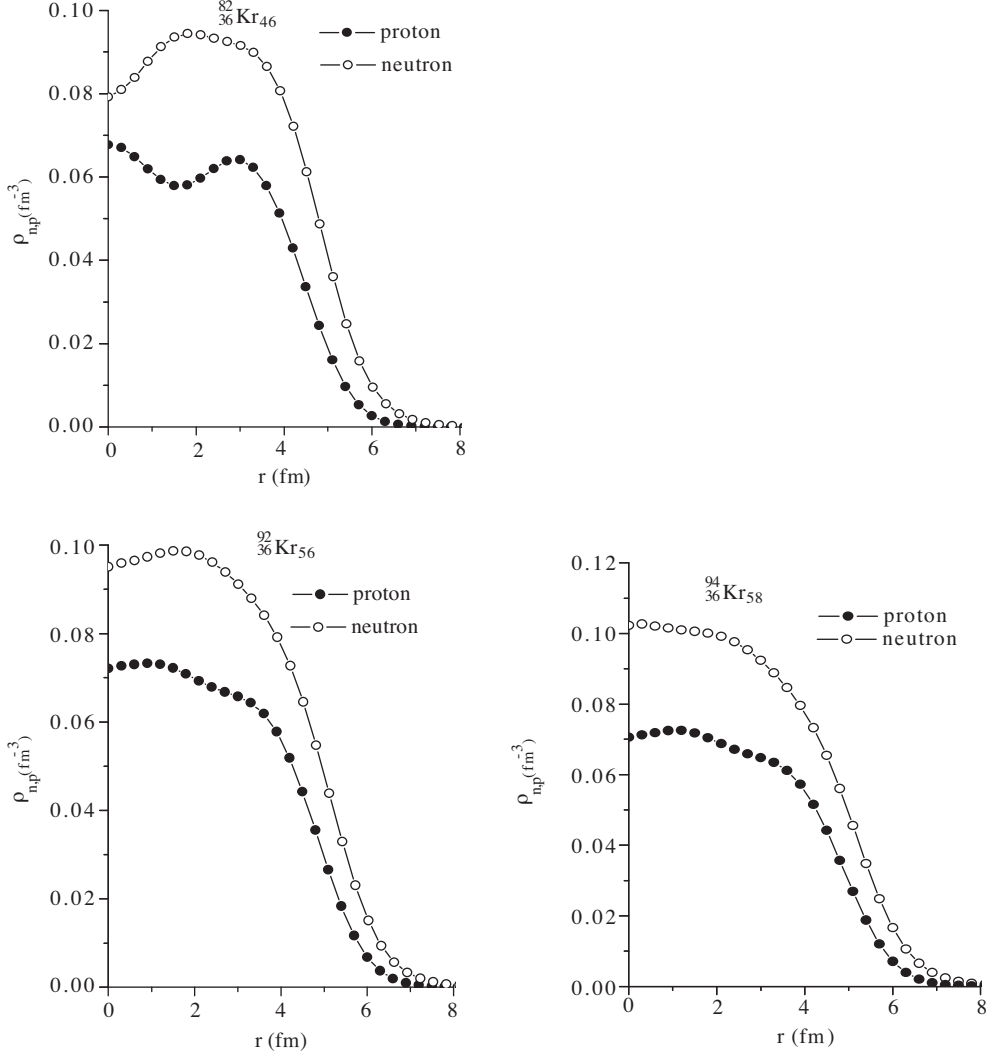
Figure 2. Comparison of calculated neutron and proton densities of Kr isotopes using the SKM* parameter.

We calculated the nuclear mass rms radii using Hartree-Fock with Skyrme forces parameters for Ni, Kr and Sn isotopes without discriminating the neutron and proton, and these radii are shown in Table 3. Like nuclear charge rms radii, the calculated with Skyrme force nuclear mass rms radii of Ni, Kr and Sn isotopes increase with increasing mass number A.

Proton rms radii calculated with the Skyrme Hartree-Fock model are shown in Table 4. It can be said that the values of charge-rms radii calculated for all Skyrme parameters (in Table 2) are larger than those of the proton rms radii (shown in Table 4).

The calculated neutron rms radii and the neutron skin thickness t with Skyrme Hartree-Fock model are given in Table 5. Note the neutron rms radii values increased with neutron number. Calculated neutron skin thickness t values from equation (12) are also shown in Table 5. Note that the neutron skin thickness t values increased from 0.879 fm (for ^{58}Ni) to 0.997 fm (for ^{64}Ni) with increasing the neutron number; but decreased to 0.880 fm for ^{78}Ni with SKM* calculations. Also, the neutron skin thickness t values increased from 0.914 fm (for ^{82}Kr) to 1.107 fm (for ^{94}Kr) by increasing neutron number. As with Ni isotopes, t values increased from 0.982 fm (for ^{109}Sn) to 1.00 fm (for ^{121}Sn) by increasing the neutron number, but decreased to 0.982 fm for ^{125}Sn with SKM* calculations.
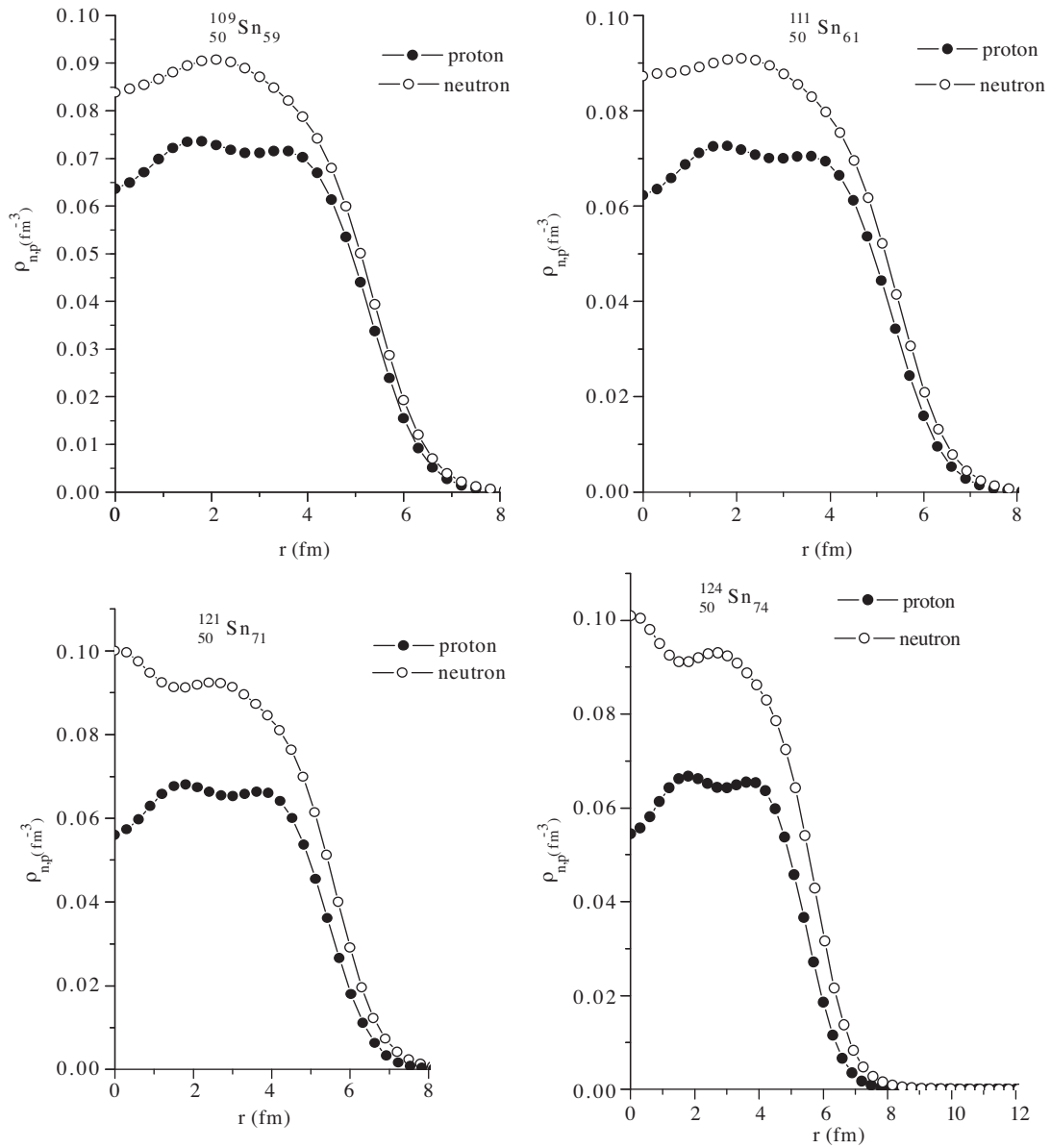
Figure 3. Comparison of calculated neutron and proton densities of Sn isotopes using the SKM* parameter.
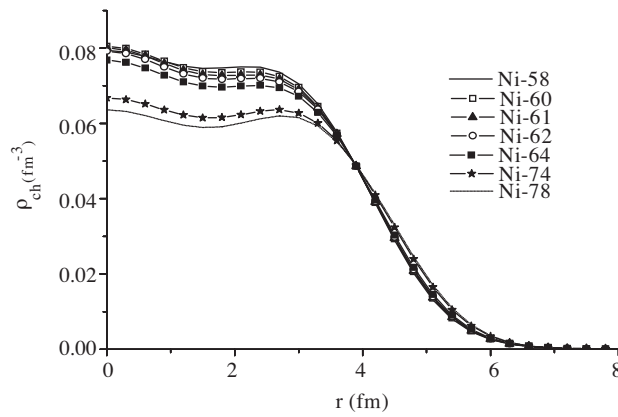
Figure 4. Comparison of charge densities of Ni isotopes calculated using the SKM* parameter.

Table 4. Calculated Root-Mean-Square (RMS) Nuclear Proton Radii.

Isotopes	SI	SIII	SVI	T3	SKM	SKM*
$^{58}\text{Ni}_{30}$	3.633	3.747	3.752	3.702	3.697	3.720
$^{60}\text{Ni}_{32}$	3.656	3.771	3.775	3.719	3.714	3.737
$^{61}\text{Ni}_{33}$	3.670	3.785	3.791	3.730	3.726	3.748
$^{62}\text{Ni}_{34}$	3.683	3.797	3.803	3.740	3.738	3.759
$^{64}\text{Ni}_{36}$	3.709	3.820	3.827	3.762	3.763	3.784
$^{74}\text{Ni}_{46}$	3.815	3.921	3.931	3.860	3.865	3.884
$^{78}\text{Ni}_{50}$	3.849	3.956	3.966	3.896	3.898	3.916
$^{82}\text{Kr}_{46}$	4.020	4.138	4.143	4.077	4.090	4.110
$^{92}\text{Kr}_{56}$	4.106	4.227	4.233	4.150	4.159	4.178
$^{94}\text{Kr}_{58}$	4.125	4.248	4.254	4.168	4.178	4.196
$^{109}\text{Sn}_{59}$	4.412	4.550	4.556	4.474	4.480	4.499
$^{111}\text{Sn}_{61}$	4.430	4.569	4.575	4.491	4.499	4.518
$^{121}\text{Sn}_{71}$	4.507	4.647	4.655	4.568	4.580	4.598
$^{124}\text{Sn}_{74}$	4.529	4.669	4.679	4.589	4.600	4.618
$^{125}\text{Sn}_{75}$	4.536	4.676	4.687	4.596	4.607	4.625

Table 5. Calculated Root-Mean-Square (RMS) Nuclear Neutron Radii and the neutron skin thickness *t* of Be isotopes with SKM* parameter.

Isotopes	SI	SIII	SVI	T3	SKM	SKM*	t
$^{58}\text{Ni}_{30}$	3.627	3.742	3.741	3.704	3.697	3.717	0.8796
$^{60}\text{Ni}_{32}$	3.685	3.802	3.798	3.767	3.760	3.780	0.9538
$^{61}\text{Ni}_{33}$	3.716	3.833	3.829	3.800	3.794	3.813	0.9760
$^{62}\text{Ni}_{34}$	3.744	3.860	3.856	3.831	3.827	3.846	0.9884
$^{64}\text{Ni}_{36}$	3.797	3.913	3.908	3.893	3.890	3.908	0.9971
$^{74}\text{Ni}_{46}$	4.009	4.134	4.122	4.144	4.130	4.148	0.9218
$^{78}\text{Ni}_{50}$	4.074	4.205	4.190	4.228	4.206	4.222	0.8802
$^{82}\text{Kr}_{46}$	4.081	4.205	4.202	4.176	4.178	4.196	0.9143
$^{92}\text{Kr}_{56}$	4.292	4.428	4.411	4.416	4.412	4.428	1.061
$^{94}\text{Kr}_{58}$	4.334	4.473	4.453	4.469	4.466	4.480	1.107
$^{109}\text{Sn}_{59}$	4.430	4.569	4.566	4.515	4.517	4.533	0.9822
$^{111}\text{Sn}_{61}$	4.464	4.605	4.601	4.555	4.557	4.574	0.9902
$^{121}\text{Sn}_{71}$	4.614	4.764	4.755	4.738	4.737	4.753	1.003
$^{124}\text{Sn}_{74}$	4.656	4.808	4.798	4.786	4.783	4.798	0.9802
$^{125}\text{Sn}_{75}$	4.669	4.821	4.812	4.801	4.797	4.812	0.9829

The neutron and proton densities for the Ni, Kr and Sn isotopes using the SKM* are shown in Figures 1–3. While the obtained values of the proton density for the Ni isotopes at the center ($r = 0$) have approximately decreased from 0.075–0.080 fm^{-3} (for ^{58}Ni) to 0.060–0.065 fm^{-3} (for ^{78}Ni) with increasing neutron number, neutron density has not changed from about 0.080–0.085 fm^{-3} (as illustrated in Figure 1). Also, proton densities for Kr isotopes, in the center, have remained approximately constant at about 0.065–0.075 fm^{-3}, but the neutron density increased from 0.075–0.080 fm^{-3} (for ^{82}Kr) to 0.100–0.105 fm^{-3} (for ^{94}Kr), as shown in Figure 2. The proton densities for Sn isotopes, at the center, remain approximately constant at about 0.055–0.065 fm^{-3}, and the neutron density remained constant at about 0.090–0.100 fm^{-3} (see Figure 3).

According to the Shell Model, the final four shell protons of Kr isotopes are in the $1f_{5/2}$ sub-shell and these nuclei are far away from closed-shell configurations for protons. Ni and Sn isotopes have magic proton number 28 and 50, respectively. That is, the $1f_{7/2}$ sub-shell level and $1g_{9/2}$ level are completely filled by protons for Ni and Sn nuclei, respectively. For neutrons, only ^{94}Kr nuclei exhibit spherical properties due to sub-shell $1g_{7/2}$ being filled completely by neutrons. ^{82}Kr and ^{92}Kr isotopes are far away from closed-shell configurations for neutrons. The $2p_{3/2}$ sub-shell level and $1g_{9/2}$ level are completely filled by neutrons for ^{60}Ni and ^{78}Ni nuclei, respectively. Also, ^{78}Ni nuclei have double magic number ($Z = 28$, $N = 50$). ^{58}Ni, ^{61}Ni, ^{62}Ni, ^{64}Ni and ^{74}Ni nuclei have not closed-shell configurations for neutrons. All Sn isotopes, which are under investigation, have not the neutron number of a closed sub-shell.

We also draw comparison with the charge densities of Ni, Kr and Sn isotopes calculated using the SKM* parameters, in Figures 4–6. The center charge density for all Ni isotopes change from about 0.06 fm^{-3} to about 0.08 fm^{-3} in Figure 4. The charge density range for all Ni isotopes from center to surface have about 6.5–7.5 fm. The charge density for all Ni isotopes have a minimum value at about 1.5–2.5 fm in Figure 4. The charge density for all Kr isotopes at center have changed from about 0.065 fm^{-3} to about 0.07 fm^{-3}, as shown in Figure 5. The charge density range for all Kr isotopes from center to surface have about 6.5–7.5 fm (only ^{82}Kr about 6.5–7.0 fm); while the charge density for ^{92}Kr and ^{94}Kr nuclei have a maximum value at about 1.0–2.0 fm. For ^{82}Kr it has a minimum value about 1.0– 2.0 fm, as shown in Figure 5. The charge density for all Sn isotopes at center have changed from about 0.06 fm^{-3} to about 0.07 fm^{-3}, as illustrated in Figure 6. The charge density range for all Sn isotopes from center to surface have chnaged about 7.5–8.0 fm. This value have a maximum value at about 1.5– 2.5 fm, as shown in Figure 6.
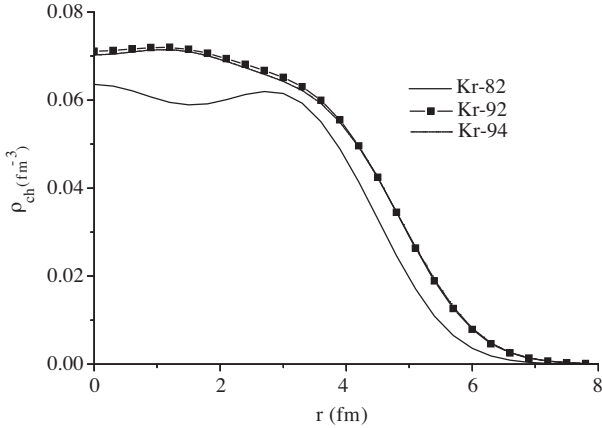
Figure 5. Comparison of charge densities of Kr isotopes calculated using the SKM* parameter.
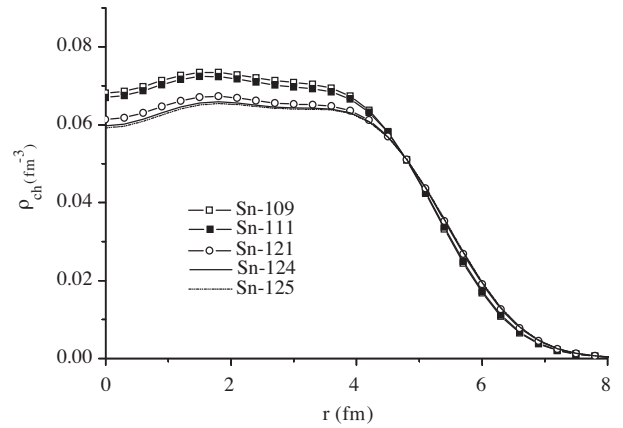
Figure 6. Comparison of charge densities of Sn isotopes calculated using the SKM* parameter.

4. Conclusions

The results calculated in SIII, T3, SKM and SKM* via Hartree-Fock method on charge radii are in good agreement with the available experimental values [21] for ^{92}Kr and ^{94}Kr; ^{60}Ni and ^{61}Ni; ^{58}Ni, ^{64}Ni, ^{121}Sn and ^{125}Sn; and ^{62}Ni, ^{82}Kr, ^{109}Sn, ^{111}Sn and ^{124}Sn, respectively. A more detailed study on rms radii of these nuclei is required when future experiments are performed. The behavior of the charge radii for Ni, Kr and Sn isotopes shows an increase of r_{char} with increase in neutron number, while the nuclear matter radii for these isotopes exhibit a faster increase. In order to test the theoretical predictions for the charge and matter radii, it is desirable to measure both matter and charge distributions for the same nuclei. The difference in size of these distributions will be of great interest and importance for theoretical understanding of the exotic nuclei structure.

References

[1] I. Tanihata, *Prog. Part Nucl. Phys.,* **35**, (1995), 505.

[2] H. Geissel, G. Münzenberg and K. Riisager, *Annu. Rev. Nucl. Part. Sci.,* **45**, (1995), 163.

[3] A. Mueller, *Prog. Part. Nucl. Phys.,* **46**, (2001), 359.

[4] Z. Wang, Z. Ren and Y. Fan, *Phys. Rev.,* **C73**, (2006), 014610.

[5] Radioactive Nuclear Beam Facilities, NuPECC Report, Europe, 2000.

[6] R. Hofstadter, *Rev. Mod. Phys.,* **28**, (1956), 214.

[7] T. W. Donnelly and I. Sick, *Rev. Mod. Phys.,* **56**, (1984), 461.

[8] H. De Vries, C. W. De Jager and C. De Vries, *At. Data Nucl. Data Tables*, **39**, (1998), 281.

[9] T. Suda, K. Maruyama and I. Tahinata, *RIKEN Accel. Prog. Rep.,* **34**, (2001), 49.

[10] An International Accelerator Facility for Beams of Ions and Antiprotons, GSI report, 2002.

[11] T. Suda, Challenges of Nuclear Structure, Proceedings of the 7th International Spring Seminar on Nuclear Physics, edited by Aldo Covello (World Scientific Publishing Co., Singapore, 2002), 13; Proposal for RIKEN RI Beam Factory, 2001.

[12] P. G. Reinhard and R. Y. Cusson, *Nucl. Phys.,* **A378**, (1982), 418.

[13] T. H. R. Skyrme, *Phil. Mag.,* **1**, (1956), 1043.

[14] M. Brack, C. Guet and H. B. Hakasson, *Phys.Rep.,* **123**, (1985), 275.

[15] L. G. Qiang, *J. Phys.,* **G17,** (1991), 1.

[16] P. Ring and P. Schuck, The Nuclear Many Body Problem, Springer, Berlin, Heidelberg, 1980.

[17] P. G. Reinhard, F. Grümmer and K. Goeke, *Z. Phys.,* **A317**, (1984), 339.

[18] http://phys.lsu.edu/graceland/faculty/cjohnson/skhafo.f

[19] B. Dreher, J. Friedrich, K. Merle, G. Lührs and H. Rothaas, *Nucl. Phys.,* **A235,** (1974), 219.

[20] B. A. Brown, *Phys. Rev.,* **C58**, (1998), 220.

[21] I. Angeli, *Atom. Data and Nucl. Data Tab.*, **87**, (2004), 185.